



HAL
open science

Aerial Oxidation of Phenol/Catechol in the Presence of Catalytic Amounts of $[(Cl)_2Mn(RCOOET)]$, $RCOOET =$ Ethyl-5-Methyl-1-(((6-Methyl-3-Nitropyridin-2-yl)Amino)Methyl)-1H-Pyrazole-3-Carboxylate

Mohamed El Boutaybi, Abderrahim Titi, Abdullah y A Alzahrani, Zahra Bahari, Monique Tillard, Belkheir Hammouti, Rachid Touzani

► **To cite this version:**

Mohamed El Boutaybi, Abderrahim Titi, Abdullah y A Alzahrani, Zahra Bahari, Monique Tillard, et al.. Aerial Oxidation of Phenol/Catechol in the Presence of Catalytic Amounts of $[(Cl)_2Mn(RCOOET)]$, $RCOOET =$ Ethyl-5-Methyl-1-(((6-Methyl-3-Nitropyridin-2-yl)Amino)Methyl)-1H-Pyrazole-3-Carboxylate. *Catalysts*, 2022, 12 (12), pp.1642. 10.3390/catal12121642 . hal-03924832

HAL Id: hal-03924832

<https://hal.science/hal-03924832>






Submitted on 5 Jan 2023

HAL is a multi-disciplinary open access archive for the deposit and dissemination of scientific research documents, whether they are published or not. The documents may come from teaching and research institutions in France or abroad, or from public or private research centers.

L'archive ouverte pluridisciplinaire **HAL**, est destinée au dépôt et à la diffusion de documents scientifiques de niveau recherche, publiés ou non, émanant des établissements d'enseignement et de recherche français ou étrangers, des laboratoires publics ou privés.

Article

Aerial Oxidation of Phenol/Catechol in the Presence of Catalytic Amounts of $[(Cl)_2Mn(RCOOET)]$, RCOOET = Ethyl-5-Methyl-1-(((6-Methyl-3-Nitropyridin-2-yl)Amino)Methyl)-1H-Pyrazole-3-Carboxylate

Mohamed El Boutaybi ^{1,*}, Abderrahim Titi ², Abdullah Y. A. Alzahrani ³, Zahra Bahari ¹, Monique Tillard ⁴, Belkheir Hammouti ² and Rachid Touzani ^{2,*}

- ¹ Laboratory of Molecular Chemistry Materials and Environment (LMCME), Multidisciplinary Faculty of Nador, University Mohammed Premier, Oujda 60000, Morocco
- ² Laboratory of Environment and Applied Chemistry (LEAC), Faculty of Sciences, University Mohammed Premier, Oujda 60000, Morocco
- ³ Department of Chemistry, Faculty of Science and Arts, King Khalid University, Mohail Assir 62529, Saudi Arabia
- ⁴ ICGM, University of Montpellier, CNRS, ENSCM, 34095 Montpellier, France
- * Correspondence: m.elboutaybi@ump.ac.ma (M.E.B.); r.touzani@ump.ac.ma (R.T.); Tel.: +212-(0)-607484225 (M.E.B.)



Citation: Boutaybi, M.E.; Titi, A.; Alzahrani, A.Y.A.; Bahari, Z.; Tillard, M.; Hammouti, B.; Touzani, R. Aerial Oxidation of Phenol/Catechol in the Presence of Catalytic Amounts of $[(Cl)_2Mn(RCOOET)]$, RCOOET = Ethyl-5-Methyl-1-(((6-Methyl-3-Nitropyridin-2-yl)Amino)Methyl)-1H-Pyrazole-3-Carboxylate. *Catalysts* **2022**, *12*, 1642. <https://doi.org/10.3390/catal12121642>

Academic Editor: Vladimir Sobolev

Received: 2 November 2022

Accepted: 10 December 2022

Published: 14 December 2022

Publisher's Note: MDPI stays neutral with regard to jurisdictional claims in published maps and institutional affiliations.



Copyright: © 2022 by the authors. Licensee MDPI, Basel, Switzerland. This article is an open access article distributed under the terms and conditions of the Creative Commons Attribution (CC BY) license (<https://creativecommons.org/licenses/by/4.0/>).

Abstract: In this work, we report on the catalytic activity of a manganese complex $[(Cl)_2Mn(RCOOET)]$, where RCOOET is ethyl-5-methyl-1-(((6-methyl-3-nitropyridin-2-yl)amino)methyl)-1H-pyrazole-3-carboxylate, in the oxidation of phenol or catechol by atmospheric oxygen to form o-quinone. The $[(Cl)_2Mn(RCOOET)]$ catalyzes the oxidation of catechol at a rate of $3.74 \mu\text{mol L}^{-1} \text{min}^{-1}$ in tetrahydrofuran (THF), in a similar manner to catecholase or tyrosinase.

Keywords: (nitropyridin-2-yl)(aminomethyl)-1H-pyrazole substituted-complex $[(Cl)_2Mn(RCOOET)]$; catecholase/tyrosinase catalytic activity; catechol; phenol

1. Introduction

Oxidation is one of the fundamental reactions of organic synthesis. In the bulk chemical industries, molecular oxygen is used as the primary oxidant owing to its economic considerations and environmental compatibility [1–5]. Efficient oxygen transport and aerobic metabolism are very crucial in most living organisms, and these are accomplished by iron or copper-containing metalloproteins [6]. The copper-containing metalloproteins have homeostatic functions such as providing defense (as antioxidants) against reactive oxygen species and pigment formation. The copper-containing metalloproteins can be divided into three groups, which contain different kinds of active sites based on their spectroscopic characteristics [7–11]: type 1 (blue), type 2 (normal), and type 3 (binuclear). The type 2 and 3 copper active sites form a trinuclear cluster, which is found in all structurally known multicopper oxidases, and this cluster is the site for oxygen binding and oxidation [12,13].

In the present study, two enzymatic oxidative transformations are discussed, i.e., those catalyzed by catecholase or tyrosinase. Catecholase is a lesser-known member of the type 3 copper-containing metalloproteins [14]. Using molecular oxygen, catecholase catalyzes the oxidation of a wide range of o-diphenols to their respective o-quinones, for which two electrons are transferred [15]. The catalytic activity of catecholase has been extensively investigated by modeling the active sites and incorporating various metals, namely copper [16–29], iron [30–33], cobalt [34–38], manganese [39–50], and zinc [51]. Mn(II) better catalyzes the oxidation reaction of phenol to o-quinone, that is why our work focuses on this kind of metal. Tyrosinase catalyzes two different reactions [52,53],

namely the hydroxylation of monophenols to dihydroxyphenylalanine and the oxidation of *o*-diphenols to *o*-quinones.

This study discusses the development of a new catechol oxidase metalloenzyme, mimetic complex $[(Cl)_2Mn(RCOOET)]$, for the catalytic oxidation of catechol or phenol to *o*-quinones. The manganese(II) complex catalyzed the catechol's oxidation, and its catalytic activity increased with the reaction time with a rate of $3.74 \mu\text{mol L}^{-1} \text{min}^{-1}$ in THF.

2. Results and Discussion

2.1. Crystal Structure of $C_{14}H_{17}N_5O_4$ (RCOOET)

The triclinic $P\bar{1}$ unit cell of $C_{14}H_{17}N_5O_4$ contains two molecules symmetry-related by the inversion center. The main crystalline characteristics and refinement data are reported in Table 1. The full results are available in a CIF file by giving the CCDC number 2178103 at the Cambridge Crystallographic Data Center [54].

Table 1. Crystal data and structure refinement for $C_{14}H_{17}N_5O_4$.

Formula	$C_{14}H_{17}N_5O_4$
CCDC	1912583
Space group,	$P\bar{1}$
Z, Formula weight	2, 318.33
Temperature (K)	298 (2)
Lattice (\AA , $^\circ$)	$a = 6.8641(3)$, $b = 11.2751(6)$, $c = 11.6535(6)$ $\alpha = 112.886(2)$, $\beta = 104.104(2)$, $\gamma = 99.536(2)$
Volume (\AA^3)	770.87(7)
Crystal (mm)	$0.14 \times 0.14 \times 0.30$
Recorded/unique reflections	21,566/3384 [$R_{\text{int}} = 0.0354$]
Goodness-of-fit on F^2	1.017
Final R1, wR2 indices [$I > 2\sigma(I)$]	0.059, 0.1489
$\Delta\rho$ Fourier residuals ($e.\text{\AA}^{-3}$)	0.25/−0.26

The structure of the RCOOET complementary moieties of the molecules of the ligand are arranged in two planes which are at an angle of about 66.8° (Figure 1). The first plane contains N3 and the methyl nitropyridinyl atoms, while the second contains the rest of the molecule. The deviation of atoms from their mean plane does not exceed 0.004\AA . The packing of the molecules in the crystal is stabilized by hydrogen-type intermolecular bonding. The current structural data brings an improvement to the previous structural report [55].

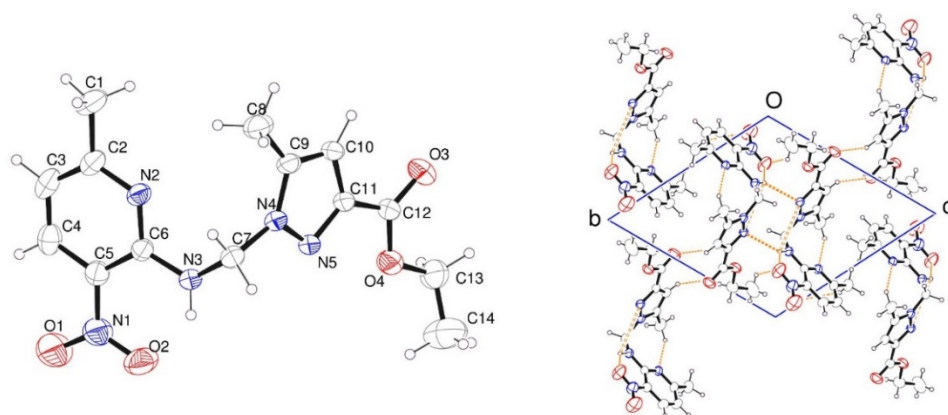


Figure 1. Ortep representation of RCOOET (the free ligand) and packing in the triclinic cell.

2.2. IR Analysis

Figure 2 exhibits the important spectral bands of the ligand and its metal complex. The IR spectra of both the ligand and the complex show a band in the zone of 3365 cm^{-1} ,

which corresponds to the N–H band. Other bands at 1711 cm^{-1} , 1644 cm^{-1} , and 1583 cm^{-1} are assigned to the C=O, C=N and C=C vibrations, respectively. The strong and sharp vibrational peak at 1491 cm^{-1} is due to C–NO₂, while in the Mn complex, C–O and C–N bands are localized at 1249 cm^{-1} and 1100 cm^{-1} , respectively. Moreover, the presence of a weak broad band at 542 cm^{-1} in the IR spectrum of the complex suggests the coordination of the ligand to the Mn(II) ion.

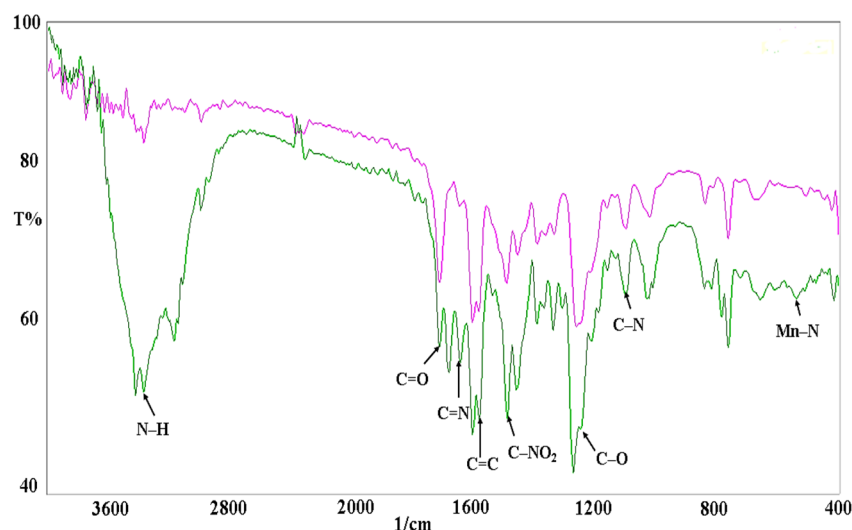


Figure 2. FT-IR spectra of: (pink) the ligand (RCOOET) and (green) [(Cl)₂Msdn(RCOOET)].

2.3. Thermal Analysis

TGA and DTA were performed to monitor the thermal stability of the ligand and its Mn complex. The temperature was increased from room temperature to $950\text{ }^{\circ}\text{C}$, at a rate of $10\text{ }^{\circ}\text{C}/\text{min}$ under a nitrogen atmosphere. The resulting TGA and DTA thermal curves for the manganese complex are shown in Figure 3.

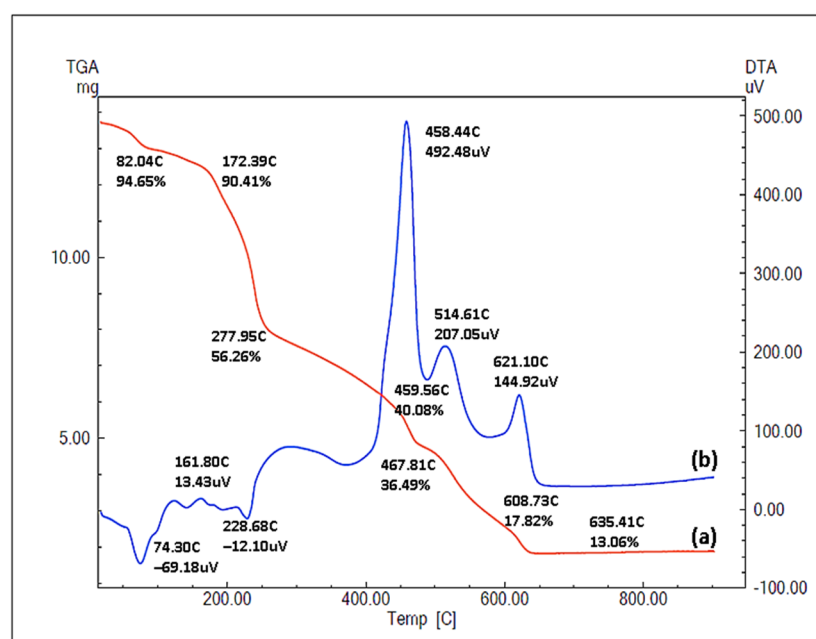


Figure 3. (a) TGA and (b) DTA curves for [(Cl)₂Mn(RCOOET)].

The mass losses and the respective gaseous (volatile) product obtained from the TGA curves are collected in Table 2 with the species proposed as mass loss. As can be seen in

the table, at higher temperatures the complex undergoes further decomposition in several stages, with the loss of one or more fragments.

Table 2. Mass losses.

Compound	Temperature (°C)	Mass Loss (%)	Proposed Lost Species
Cl ₂ MnRCOOET	0–82	5.35	Solvent
	82–172	4.24	Chlorine
	172–278	16.18	C ₅ H ₅ N ₂
	278–467	19.77	C ₃ H ₅ O ₂
	467–635	23.43	C ₅ H ₆ N ₃

2.4. Catecholase Mimicking Activity of [(Cl)₂Mn(RCOOET)]

The catecholase-mimicking activity of [(Cl)₂Mn(RCOOET)] towards catechol oxidation in aerated THF (saturated with molecular oxygen) was investigated spectrophotometrically by following the absorption of the corresponding o-quinone at 390 nm over time. The evolution of the absorption of o-quinone in the presence of the complex prepared in situ in THF and the synthesized complex in THF is shown schematically in Figure 4.

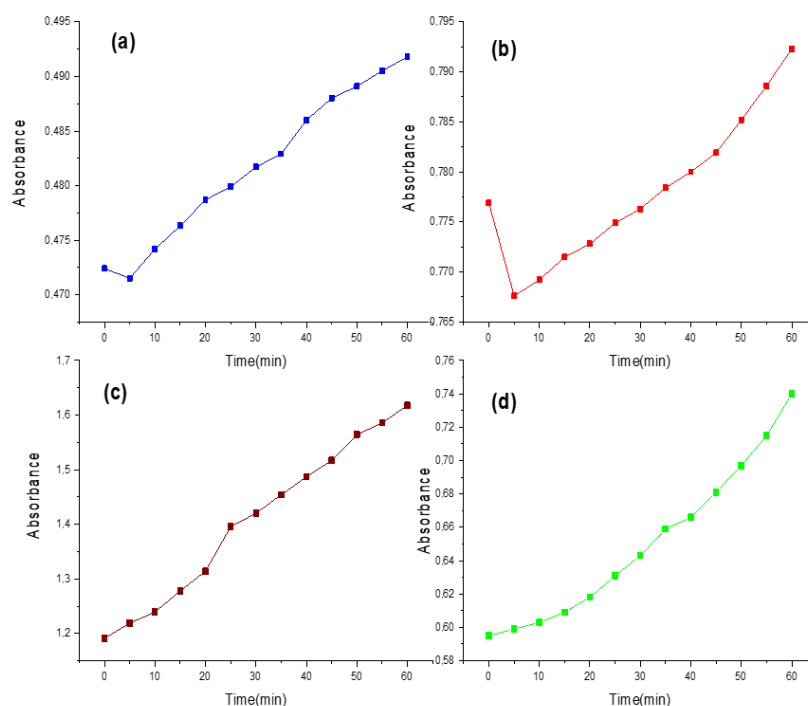


Figure 4. Absorption reading at 390 nm accompanying the [(Cl)₂Mn(RCOOET)]-catalyzed oxidation of catechol to o-quinone, (a) [(Cl)₂Mn(RCOOET)] formed in situ in MeOH, (b) pre-synthesized [(Cl)₂Mn(RCOOET)] in MeOH, (c) pre-synthesized [(Cl)₂Mn(RCOOET)] in THF and (d) [(Cl)₂Mn(RCOOET)] formed in situ in THF.

Figure 5 shows the UV-visible spectrum of the absorption of o-quinone in the presence of the synthesized complex in THF. It is clear that no peak occurs when catechol is used alone, and that the intensity of the absorption peak of o-quinone at 390 nm increases due to the presence of the synthesized complex in the catechol solution. The evolution of o-quinone absorption was followed up for 3 h, and the spectra were recorded every 30 min.

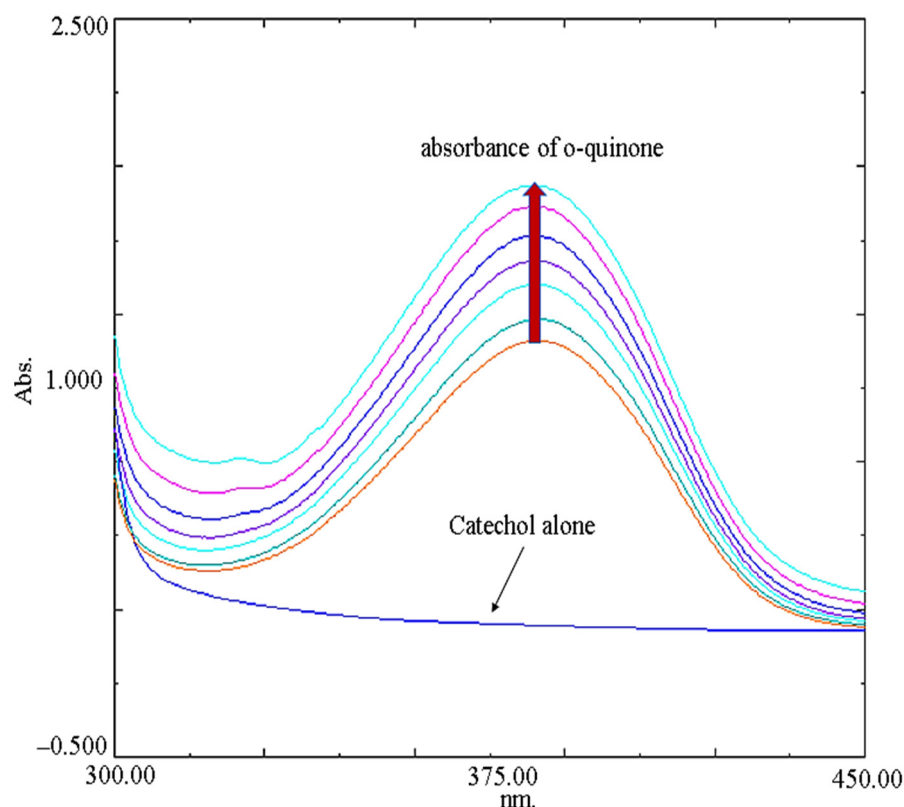


Figure 5. UV-visible spectra of absorbance of o-quinone from the oxidation of catechol in the presence of the $[(Cl)_2Mn(RCOOET)]$ in THF.

In both cases, it was observed that the absorbance of o-quinone increased with time, indicating that $[(Cl)_2Mn(RCOOET)]$ catalyzed the aerial oxidation of catechol to o-quinone over time. To understand the effect of the solvent, similar experiments were run under the same thermodynamic conditions with MeOH as the solvent. Again, the aerial oxidation of catechol in the presence of the Mn(II) complex was evidenced by the evolution of the absorption of o-quinone in the presence of the synthesized complex in MeOH or the in situ prepared complex in MeOH, and this is shown schematically in Figure 4. The calculated catechol oxidation rates are reported in Table 3. It is observed that the rate of oxidation of catechol in THF is higher ($v = 3.74 \mu\text{mol L}^{-1} \text{min}^{-1}$). It can be speculated that THF showed excellent catalytic activity for the oxidation of catechol to o-quinone. Polar solvents such as THF can strongly solvate Cl^- anions by creating hydrogen bonds. Furthermore, THF is a good σ donor and poor π acceptor.

Table 3. Oxidation rate of $[(Cl)_2Mn(RCOOET)]$ catalyzed oxidation of catechol ($\mu\text{mol.L}^{-1}.\text{min}^{-1}$).

Solvent	Complex	MeOH	THF
	The synthesized complex	0.16	3.74
	the prepared complex in situ	0.2	1.51

2.5. Kinetic Study

The mechanism and the rate of the oxidation of catechol to o-quinone by dioxygen, and catalyzation by $[(Cl)_2Mn(RCOOET)]$, were studied by the method of initial rates. For the procedure, 0.3 mL of the complex solution ($2 \times 10^{-3} \text{ mol L}^{-1}$) and 2 mL of the catechol solution (concentration varied from $10^{-3} \text{ mol L}^{-1}$ to $3 \times 10^{-1} \text{ mol L}^{-1}$) were mixed together, and the absorbance of o-quinone at 390 nm was noted every 5 min. As shown in Figure 6, a plot of the initial rate, V , versus $[Catechol]$ shows saturation kinetics. To test the

enzymolysis kinetics, the Michaelis–Menten model was applied. A plot of the reciprocals of rate and [catechol] is shown in Figure 7. It is almost linear only in the concentration range 10^{-3} M– 3×10^{-1} M. The linear fit gave the kinetic parameters shown in Table 4 for the catechol oxidation in the presence of catalytic amounts of $[(\text{Cl})_2\text{Mn}(\text{RCOOET})]$. The smaller K_m is, the more maximal enzyme activity is reached for a low level of substrate concentration. The affinity of the enzyme for the substrate is high.

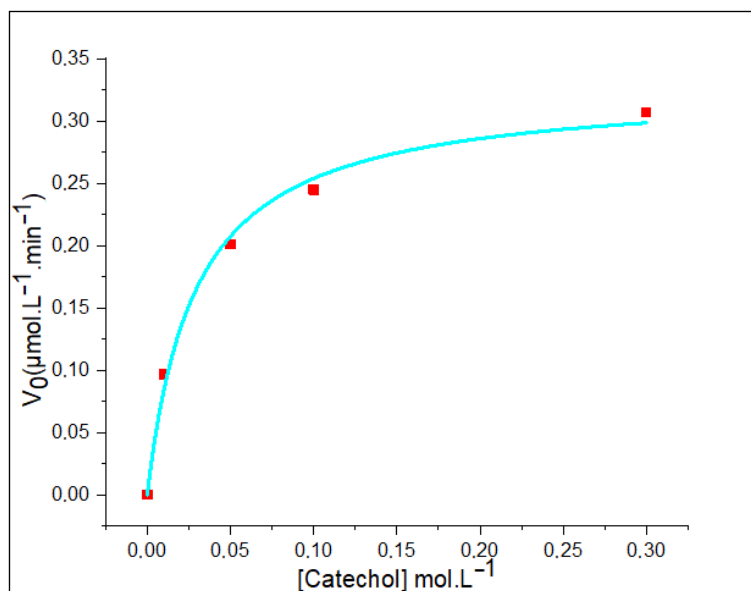


Figure 6. Correlation between reaction rate and catechol concentrations catalyzed by $[(\text{Cl})_2\text{Mn}(\text{RCOOET})]$.

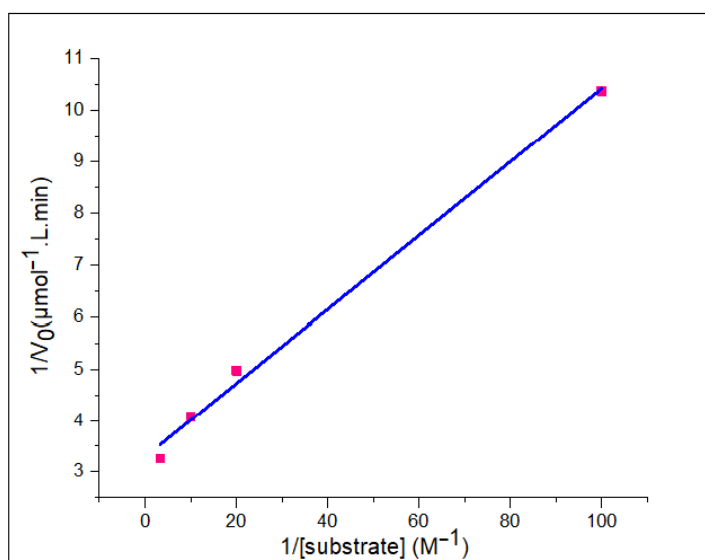


Figure 7. Lineweaver–Burk plot of $1/\text{rate}$ vs. $1/[\text{catechol}]$.

Table 4. Values of the V_{max} and K_m of the reaction catalyzed by the complex in THF.

Complex	V_{max} ($\mu\text{mol. L}^{-1} \cdot \text{min}^{-1}$)	K_m (mol. L^{-1})
$[(\text{Cl})_2\text{Mn}(\text{RCOOET})]$	0.307	0.083

2.6. Tyrosinase Mimicking Activity of $[(\text{Cl})_2\text{Mn}(\text{RCOOET})]$

To study the tyrosinase-mimicking activity of $[(\text{Cl})_2\text{Mn}(\text{RCOOET})]$ towards the aerial oxidation of phenol, a kinetic method analogous to that described for the catecholase-

mimicking activity was used, using phenol as a substrate. The evolution of the absorption of o-quinone due to the oxidation of phenol by oxygen in MeOH in the presence of the $[(Cl)_2Mn(RCOOET)]$, which had been formed in situ in MeOH or pre-synthesized, is shown schematically in Figure 8. The spectral changes indicated that the complex catalyzes the oxidation of phenol.

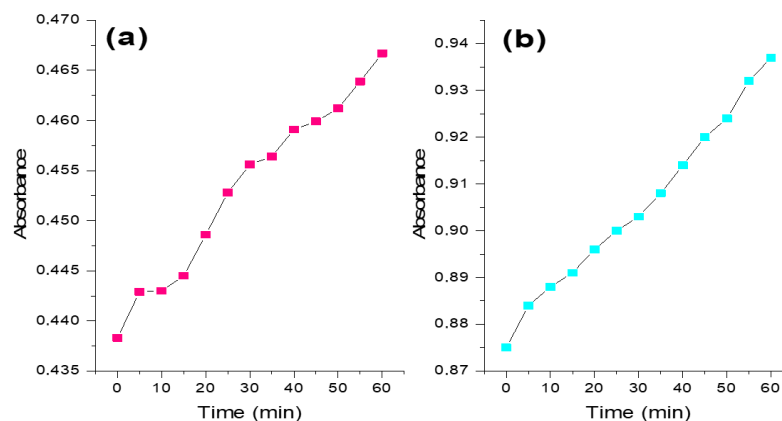


Figure 8. Phenol oxidation in the presence of (a) $[(Cl)_2Mn(RCOOET)]$ formed in situ and (b) pre-synthesized $[(Cl)_2Mn(RCOOET)]$ in MeOH.

Figure 9 shows the UV-visible overlay spectra of the absorption of o-quinone in the presence of the synthesized $[(Cl)_2Mn(RCOOET)]$ in MeOH. A peak appears at 390 nm after the addition of the complex solution to the phenol solution, and the absorbance of o-quinone increases over time. The evolution of o-quinone absorption was followed up for 2 h 30 min, and the spectra were recorded every 15 min.

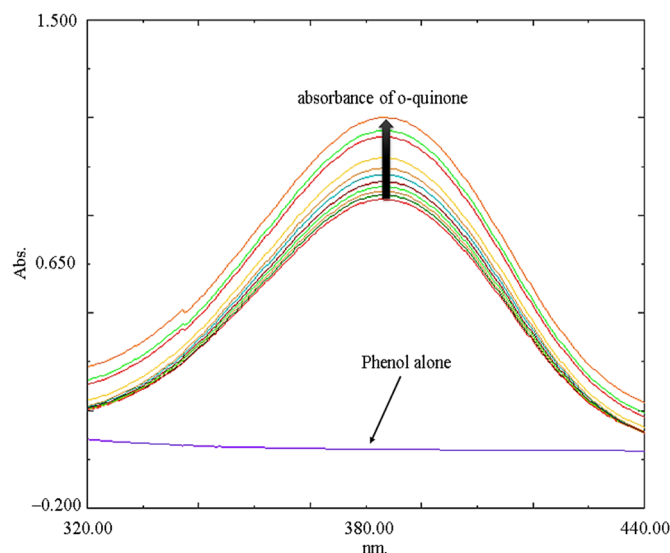
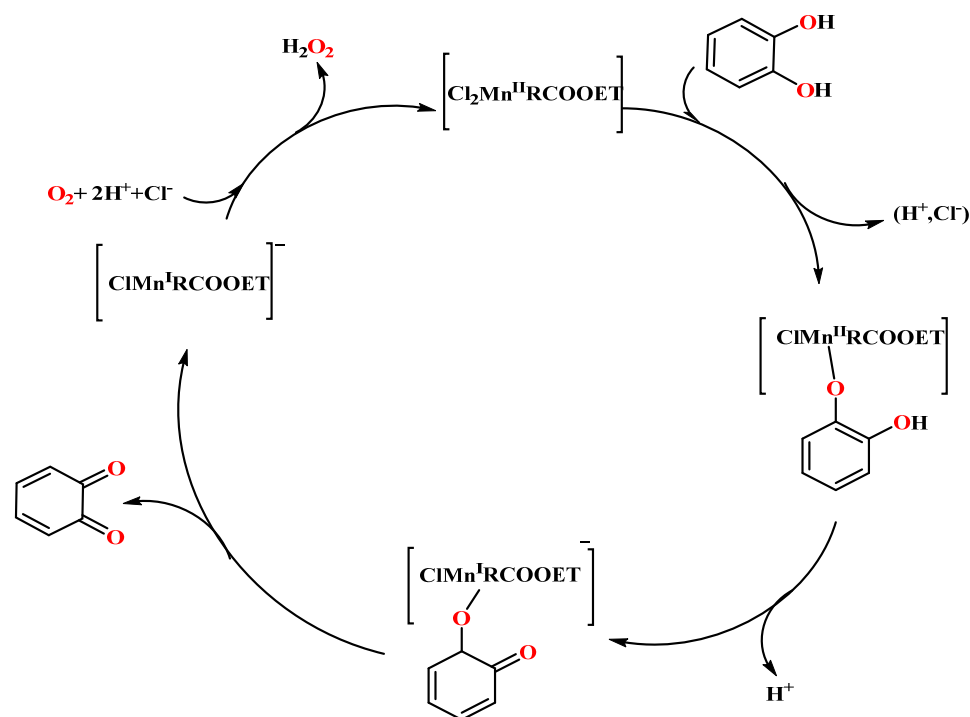


Figure 9. UV-visible spectrum of absorption of o-quinone in the presence of the pre-synthesized $[(Cl)_2Mn(RCOOET)]$ in MeOH.

2.7. Proposed Mechanism of Action of Catechol Oxidase

Different approaches have been used by different research groups to study the mechanism of complexes with catecholase-like activity. In this work, we propose that the dioxygen is reduced by catechol to hydrogen peroxide (Scheme 1). Similar to the catalyzed oxidation of catechol by catecholase, the substrate is primarily coordinated to the $[(Cl)_2Mn(RCOOET)]$ complex monodentately, and this is followed by its rapid oxidation to o-quinone and the concurrent reduction of Mn(II) to Mn(I).



Scheme 1. The proposed catalytic mechanism for the oxidation reaction of catechol.

3. Materials and Methods

3.1. Materials

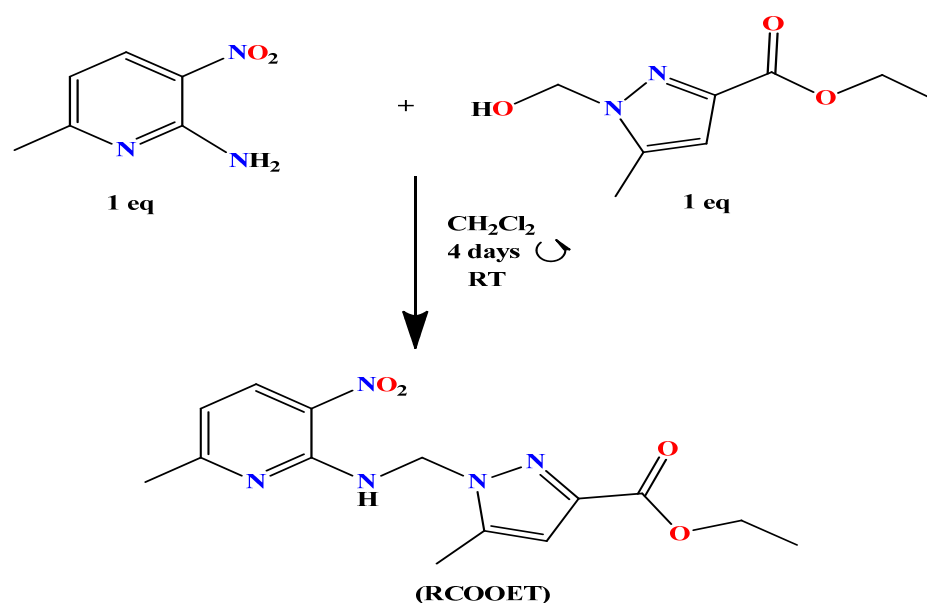
The chemicals and solvents, 6-methyl-3-nitropyridinamine (97%), methanol, acetonitrile, tetrahydrofuran, diethyl ether, dihydroxy-1,2-benzene (catechol), phenol, magnesium sulfate, dichloromethane, as well as the metal salt ($\text{MnCl}_2 \cdot 4\text{H}_2\text{O}$) were purchased from Sigma-Aldrich and used without any further purification. ^1H NMR and ^{13}C NMR spectra were recorded on a Bruker Advance Digital 400 NMR spectrometer. Chemical shifts were recorded in parts per million (ppm) using SiMe_4 (TMS) as an internal standard. The elemental analysis was conducted using a 2400 Series II CHNS/O Elemental Analyzer.

3.2. Methods

3.2.1. Synthesis of Ethyl-5-Methyl-1-(((6-Methyl-3-Nitropyridin-2-yl)Amino)Methyl)-1H-Pyrazole Carboxylate (RCOOET)

The ligand (RCOOET) was prepared by using a procedure described in the literature [56]. The solution of ethyl 1-(hydroxymethyl)-5-methyl-1H-pyrazole-3-carboxylate in CH_2Cl_2 (1 eq.) was added to the solution of 6-methyl-3-nitropyridin-2-amine in CH_2Cl_2 (1 eq.) (Scheme 2). The mixture was stirred at room temperature for 4 days and then dried over MgSO_4 . The product was recrystallized from the resultant solution using a mixture of methanol with a few drops of ether. After 3 days, the obtained yellow product was filtered and washed with methanol (2×50 mL), followed by washing with Et_2O (2×50 mL) to yield the ligand RCOOET as the final product. The structure of RCOOET is shown in Scheme 2.

Yellow product (1.5 g, 52.3% yield). mp = 454 K. FT-IR, cm^{-1} : 1100 (C-N), 1249 (C-O), 1491 (C- NO_2), 1583 (C=C), 1644 (C=N), 1711 (C=O), 3365 (N-H). UV-vis ($\lambda = 335$ nm, 347 nm, and 368 nm). ^1H NMR (400 MHz, CDCl_3): δ H = 1.40 (t, 3H, CH_3), 2.54 (s, 3H, CH_3 _{PyR}), 2.57 (s, 3H, CH_3 _{Ar}), 4.4 (q, 2H, CH_2), 5.99 (d, 2H, CH_2), 6.55 (s, 1H, C_{PyR}), 6.65 (d, 1H, CH_{Ar}), 8.33 (d, CH, CH_{Ar}), and 8.98 (t, 1H, NH). ^{13}C NMR (100 MHz, CDCl_3): δ C = 11.35 (CH_3), 14.42 (CH_3), 24.95 (CH_3), 53.73 (CH_2), 60.99 (CH_2), 108.27 (CH_{PyR}), 113.93 (CH_{Ar}), 126.53 (CH_{Ar}), 135.68 (C_{PyR}), 140.64 (C_{Ar}), 143.73 (C_{Ar}), 150.25 (C_{Ar}), 162.42 (C_{Ar}), and 165.59 (Cest). Elemental Analysis: C, 52.66%; H, 5.37%; N, 21.93% (calculated); C, 52.73%; H, 5.31%; N, 22.01% (found).



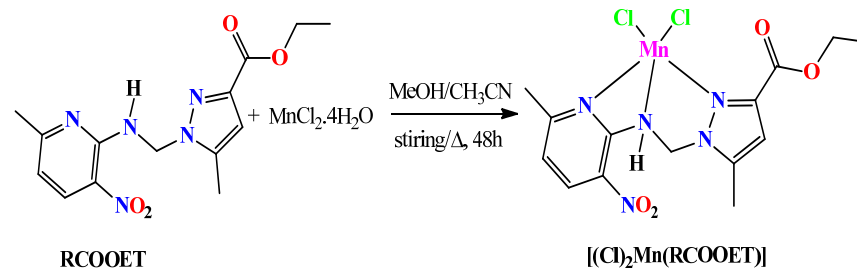
Scheme 2. Synthesis of the ligand, RCOOET.

3.2.2. X-ray Single Crystal Study of RCOOET

Yellow stick-shaped crystals of the free ligand were selected for the singularity using a stereo microscope with a polarizing filter. The measurement of diffracted intensities was performed at ambient temperature on a 4-circle diffractometer, a Bruker D8 Venture device, using a Mo micro-source (Incoatec I μ S 3.0, 110 μ m beam, K α radiation) and a Photon II CPAD detector. Reflections (27,294, up to θ max of 27.04 $^\circ$) were handled in the Apex software suite [57] and indexed in a triclinic lattice, $a = 6.8641(3)$, $b = 11.2751(6)$, $c = 11.6535(6)$ \AA , $\alpha = 112.886(2)$, $\beta = 104.104(2)$, $\gamma = 99.536(2)^\circ$. The SHELX programs were used for the structure solution and full-matrix least-square refinements [58]. Non-H atoms were considered with anisotropic displacement parameters.

3.2.3. Synthesis of [(Cl) $_2$ Mn(RCOOET)]

The solution of 1 equivalent of MnCl $_2$ ·4H $_2$ O (123.95 mg, 0.626 mmol) in 5 mL of methanol was added to a solution of 1 equivalent of RCOOET (200 mg, 0.626 mmol) in 10 mL of acetonitrile. A yellow-colored solution was filtered to remove the solid impurities. Then, the filtrate was allowed to evaporate at room temperature for more than one week to obtain a yellow powder of [(Cl) $_2$ Mn(RCOOET)]. The structure of the expected [(Cl) $_2$ Mn(RCOOET)] is shown in Scheme 3.

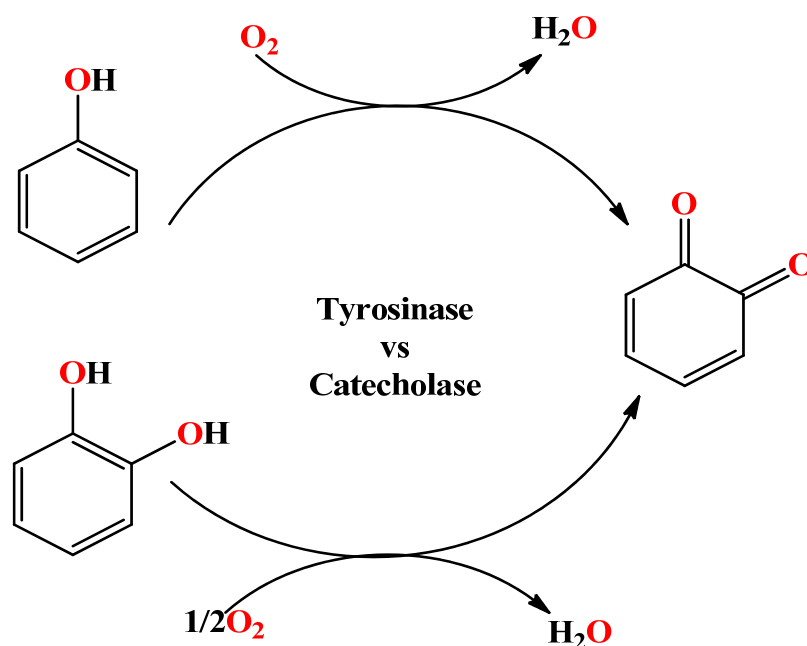


Scheme 3. Synthetic route of [(Cl) $_2$ Mn(RCOOET)].

3.2.4. Catecholase and Tyrosinase Activity of [(Cl) $_2$ Mn(RCOOET)]

The biochemical oxidation of phenol and catechol by molecular oxygen to form o-quinone is catalyzed by tyrosinase and catecholase, respectively. The general catalytic cycle is shown in Scheme 4. The synthesized complex, [(Cl) $_2$ Mn(RCOOET)], has the potential to mimic these two enzymes for the catalytic oxidation of phenols by dioxygen to form their respective quinones. To study the catecholase- and tyrosinase-mimetic activity of

$[(Cl)_2Mn(RCOOET)]$, catechol or phenol was reacted with O_2 (from the aerated solvent), in the presence of catalytic amounts of the complex. The catalytic-mimetic activity and, hence, the progress of the reactions were monitored spectrophotometrically in THF or methanol under ambient conditions. Two sets of experiments were carried out. In the first set, initially, 0.15 mL of $MnCl_2 \cdot 4H_2O$ (2 mmol) and 0.15 mL of RCOOET solution (2 mmol) were mixed in a spectrophotometric cell to prepare the complex in situ, followed by the addition of 2 mL of the substrate. In the second set, 0.3 mL of the previously prepared complex solution ($10^{-1} \text{ mol.L}^{-1}$) was mixed with 2 mL of the substrate. The evolution of the absorption of o-quinone over time (from 0 to 65 min) was noted for both sets at 390 nm using UV-Vis spectroscopy.



Scheme 4. Biochemical oxidation of phenol/catechol by catecholase (bottom) and tyrosine (top) [14].

4. Conclusions

A pyrazole-based ligand, ethyl-5-methyl-1-(((6-methyl-3-nitropyridin-2-yl)amino)methyl)-1H-pyrazole-3-carboxylate, and its complex were successfully synthesized. These compounds were analyzed using different characterization techniques, such as FTIR, DRX, and ATG-ATD, and later dual activity, mimicking the catecholase activity towards the oxidation of the catechol to o-quinone, and mimicking the tyrosinase activity towards the oxidation of phenol to catechol and then to o-quinone. The pre-synthesized $[(Cl)_2Mn(RCOOET)]$ complex showed a higher oxidation rate in THF ($3.74 \mu\text{mol.L}^{-1} \cdot \text{min}^{-1}$) than in MeOH ($0.16 \mu\text{mol.L}^{-1} \cdot \text{min}^{-1}$) for the oxidation of catechol to o-quinone, indicating that the type of solvent plays an important role in the catalytic activity of the complex.

Author Contributions: Conceptualization, R.T. and M.E.B.; methodology, M.E.B. and A.T. software, M.T.; validation, B.H. and A.T.; formal analysis, R.T. and M.E.B.; investigation, R.T.; resources, Z.B.; data curation, A.T. and M.E.B.; writing—original draft preparation, A.T. and M.E.B.; writing—review and editing, A.Y.A.A. and M.T.; supervision, R.T. and Z.B.; project administration, A.Y.A.A.; funding acquisition, A.Y.A.A. All authors have read and agreed to the published version of the manuscript.

Funding: The authors extend their appreciation to the Deanship of Scientific Research at King Khalid University for funding this work through the Large Research Project under grant number (RGP.2/191/43).

Data Availability Statement: Data available upon request from corresponding authors.

Conflicts of Interest: The authors declare no conflict of interest.

References

1. Gligorich, K.M.; Sigman, M.S. Recent advancements and challenges of palladium II-catalyzed oxidation reactions with molecular oxygen as the sole oxidant. *Chem. Commun.* **2009**, 3854–3867. [[CrossRef](#)] [[PubMed](#)]
2. Piera, J.; Backvall, J.E. Catalytic oxidation of organic substrates by molecular oxygen and hydrogen peroxide by multistep electron transfer—A biomimetic approach. *Angew. Chem. Int. Ed.* **2008**, *47*, 3506–3523. [[CrossRef](#)] [[PubMed](#)]
3. Stahl, S.S. Palladium-Catalyzed Oxidation of Organic Chemicals with O₂. *Science* **2005**, *309*, 1824–1826. [[CrossRef](#)] [[PubMed](#)]
4. Punniyamurthy, T.; Velusamy, S.J. Recent advances in transition metal catalyzed oxidation of organic substrates with molecular oxygen. *Iqbal Chem. Rev.* **2005**, *105*, 2329–2363. [[CrossRef](#)] [[PubMed](#)]
5. Stahl, S.S. Palladium oxidase catalysis: Selective oxidation of organic chemicals by direct dioxygen-coupled turnover. *Angew. Chem. Int. Ed.* **2004**, *43*, 3400–3420. [[CrossRef](#)] [[PubMed](#)]
6. Gerdemann, C.; Eicken, C.; Krebs, B. The crystal structure of catechol oxidase: New insight into the function of type-3 copper proteins. *Acc. Chem. Res.* **2002**, *35*, 183–191. [[CrossRef](#)]
7. Palm-Espling, M.E.; Niemiec, M.S.; Wittung-Stafshede, P. Role of metal in folding and stability of copper proteins in vitro. *Biochim. Biophys. Acta-Mol. Cell Res.* **2012**, *1823*, 1594–1603. [[CrossRef](#)]
8. Huffman, D.L.; O'Halloran, T.V. Function, structure, and mechanism of intracellular copper trafficking proteins. *Annu. Rev. Biochem.* **2001**, *70*, 677–701. [[CrossRef](#)]
9. Puig, S.; Thiele, D.J. Molecular mechanisms of copper uptake and distribution. *Curr. Opin. Chem. Biol.* **2002**, *6*, 171–180. [[CrossRef](#)]
10. Harris, E.D. Basic and clinical aspects of copper. *Crit. Rev. Clin. Lab. Sci.* **2003**, *40*, 547–586. [[CrossRef](#)]
11. Malmström, B.G. Enzymology of oxygen. *Annu. Rev. Biochem.* **1982**, *51*, 21–59. [[CrossRef](#)]
12. Messerschmidt, A.; Rossi, A.; Ladenstein, R.; Huber, R.; Bolognesi, M.; Gatti, G.; Marchesini, A.; Petruzzelli, R.; Finazziagro, A.J. X-ray crystal structure of the blue oxidase ascorbate oxidase from zucchini: Analysis of the polypeptide fold and a model of the copper sites and ligands. *Mol. Biol.* **1989**, *206*, 513–529. [[CrossRef](#)]
13. Spira-Solomon, D.J.; Allendorf, M.D.; Solomon, E.I. Low-temperature magnetic circular dichroism studies of native laccase: Confirmation of a trinuclear copper active site. *J. Am. Chem. Soc.* **1986**, *108*, 5318–5328. [[CrossRef](#)]
14. Solomon, E.I.; Sundaram, U.M.; Machonkin, T.E. Multicopper oxidases and oxygenases. *Chem. Rev.* **1996**, *96*, 2563–2605. [[CrossRef](#)]
15. Gerdemann, C.; Eicken, C.; Galla, H.-J.; Krebs, B.J. Comparative modeling of the latent form of a plant catechol oxidase using a molluscan hemocyanin structure. *Inorg. Biochem.* **2002**, *89*, 155–158. [[CrossRef](#)] [[PubMed](#)]
16. Patra, A.; Giri, G.C.; Sen, T.K.; Carrella, L.; Mandal, S.K.; Bera, M. Bis (μ -alkoxo) bridged dinuclear Cu^{II}₂ and Zn^{II}₂ complexes of an isoindol functionality based new ligand: Synthesis, structure, spectral characterization, magnetic properties and catechol oxidase activity. *Polyhedron* **2014**, *67*, 495–504. [[CrossRef](#)]
17. Mandal, S.; Mukherjee, J.; Lloret, F.; Mukherjee, F. Modeling Tyrosinase and Catecholase Activity Using New m-Xylyl-Based Ligands with Bidentate Alkylamine Terminal Coordination. *Inorg. Chem.* **2012**, *51*, 13148–13161. [[CrossRef](#)]
18. Biswas, A.; Das, L.K.; Drew, M.G.B.; Diaz, C.; Ghosh, A. Insertion of a hydroxido bridge into a diphenoxido dinuclear copper (II) complex: Drastic change of the magnetic property from strong antiferromagnetic to ferromagnetic and enhancement in the catecholase activity. *Inorg. Chem.* **2012**, *51*, 10111–10121. [[CrossRef](#)]
19. Agotegaray, M.A.; Dennehy, M.; Boeris, M.A.; Grela, M.A.; Burrow, R.A.; Quin-zani, O.V. Therapeutic properties, SOD and catecholase mimetic activities of novel ternary copper (II) complexes of the anti-inflammatory drug Fenoprofen with imidazole and caffeine. *Polyhedron* **2012**, *34*, 74–83. [[CrossRef](#)]
20. Sadhukhan, D.; Ray, A.; Butcher, R.J.; Gomez Garcia, C.J.; Dede, B.; Mitra, S. Magnetic and catalytic properties of a new copper (II)–Schiff base 2D coordination polymer formed by connected helical chains. *Inorg. Chim. Acta* **2011**, *376*, 245–254. [[CrossRef](#)]
21. Panda, M.K.; Shaikh, M.M.; Butcher, R.J.; Ghosh, P. Functional mimics of catechol oxidase by mononuclear copper complexes of sterically demanding [NNO] ligands. *Inorg. Chim. Acta* **2011**, *372*, 145–151. [[CrossRef](#)]
22. Majumder, S.; Sarkar, S.; Sasmal, S.; Sanudo, E.C.; Mohanta, S. Heterobridged dinuclear, tetranuclear, dinuclear-based 1-D, and heptanuclear-based 1-D complexes of copper (II) derived from a dinucleating ligand: Syntheses, structures, magnetochemistry, spectroscopy, and catecholase activity. *Inorg. Chem.* **2011**, *50*, 7540–7554. [[CrossRef](#)] [[PubMed](#)]
23. Bakshi, R.; Rossi, M.; Caruso, F.; Mathur, P. Copper (II) complexes of a new N-picolylated bis benzimidazolyl diamide ligand: Synthesis, crystal structure and catechol oxidase studies. *Inorg. Chim. Acta* **2011**, *376*, 175–188. [[CrossRef](#)]
24. El Boutaybi, M.; Bouroumane, N.; Azzouzi, M.; Bacroume, S.; Touzani, R.; Bahari, Z. Catecholase, phenoxazinone synthase and copper (Cu^{II}) complex based on pyrazolic ligand: Preparation and characterization. *Mater. Today Proc.* **2022**. [[CrossRef](#)]
25. Kaddouri, Y.; Haddari, H.; Titi, A.; Yousfi, E.B.; Chetouani, A.; El Kodadi, M.; Touzani, R. Catecholase catalytic properties of copper (II) complexes prepared in-situ with heterocyclic ligands: Experimental and DFT study. *Moroc. J. Chem.* **2020**, *8*, 184–196. [[CrossRef](#)]
26. Titi, A.; Al-Noaimi, M.; Kaddouri, Y.; El Ati, R.; Yousfi, E.B.; El Kodadi, M.; Touzani, R. Study of the catecholase catalytic properties of copper (II) complexes prepared in-situ with monodentate ligands. *Mater. Today Proc.* **2019**, *13*, 1134–1142. [[CrossRef](#)]
27. El Ati, R.; Takfaoui, A.; El Kodadi, M.; Touzani, R.; Yousfi, E.B.; Almalki, F.A.; Ben Hadda, T. Catechol oxidase and Copper(I/II) Complexes Derived from Bipyrazol Ligand: Synthesis, molecular structure investigation of new biomimetic functional model and mechanistic study. *Mater. Today Proc.* **2019**, *13*, 1229–1237. [[CrossRef](#)]

28. Boyaala, R.; El Ati, R.; Khoutoul, M.; El Kodadi, M.; Touzani, R.; Hammouti, B. Biomimetic oxidation of catechol employing complexes formed in situ with heterocyclic ligands and different copper(II) salts. *J. Iran. Chem. Soc.* **2018**, *15*, 85–92. [[CrossRef](#)]
29. Bouroumane, N.; El Kodadi, M.; Touzani, R.; El Boutaybi, M.; Oussaid, A.; Hammouti, B.; Nandiyanto, A.B.D. New pyrazole-based ligands: Synthesis, characterization, and catalytic activity of their copper complexes. *Arab. J. Sci. Eng.* **2021**, *47*, 269–279. [[CrossRef](#)]
30. Indira, S.; Vinoth, G.; Bharathi, M.; Bharathi, S.; Rahiman, A.K.; Bharathi, K.S. Catechol oxidase and phenoxazinone synthase mimicking activities of mononuclear Fe(III) and Co(III) complexes of aminobis(phenolate)-based mixed ligands: Synthesis, spectral and electrochemical studies. *Inorg. Chim. Acta* **2019**, *495*, 118988. [[CrossRef](#)]
31. Lo, S.-I.; Lu, J.-W.; Chen, W.-J.; Wang, S.-R.; Wei, H.-H.; Katada, M. Functional model for catecholase-like activity: Synthesis, structure, spectra, and catalytic activity of iron (III) complexes with substituted-salicylaldimine ligands. *Inorg. Chim. Acta* **2009**, *362*, 4699–4705. [[CrossRef](#)]
32. Megyes, T.; May, Z.; Schubert, G.; Grosz, T.; Simandi, L.I.; Radnai, T. Synthesis and structure study of some catecholase-mimetic iron complexes. *Inorg. Chim. Acta* **2006**, *359*, 2329–2336. [[CrossRef](#)]
33. Simandi, L.I.; Simandi, T.M.; May, Z.; Besenyey, G. Catalytic activation of dioxygen by oximatocobalt (II) and oximatoiron (II) complexes for catecholase-mimetic oxidations of o-substituted phenols. *Coord. Chem. Rev.* **2003**, *245*, 85–93. [[CrossRef](#)]
34. Majumder, S.; Mondal, S.; Lemoine, P.; Mohanta, S. Dinuclear mixed-valence Co III Co II complexes derived from a macrocyclic ligand: Unique example of a Co III Co II complex showing catecholase activity. *Dalton Trans.* **2013**, *42*, 4561–4569. [[CrossRef](#)]
35. Banerjee, A.; Guha, A.; Adhikary, J.; Khan, A.; Manna, K.; Dey, S.; Zangrando, E.; Das, D. Dinuclear cobalt (II) complexes of Schiff-base compartmental ligands: Syntheses, crystal structure and bio-relevant catalytic activities. *Polyhedron* **2013**, *60*, 102–109. [[CrossRef](#)]
36. Zhang, Y.; Meng, X.G.; Liao, Z.R.; Li, D.F.; Liu, C.L. Synthesis, structures and polyphenol oxidase activities of dicopper and dicobalt complexes. *J. Coord. Chem.* **2009**, *62*, 876–885. [[CrossRef](#)]
37. Titi, A.; Warad, I.; Tillard, M.; Touzani, R.; Messali, M.; El Kodadi, M.; Eddike, D.; Zarrouk, A. Inermolecular interaction in $[C_6H_{10}N_3]_2 [CoCl_4]$ complex: Synthesis, XRD/HSA relation, spectral and catecholase catalytic analysis. *J. Mol. Struct.* **2020**, *1217*, 128422. [[CrossRef](#)]
38. Titi, A.; Shiga, T.; Oshio, H.; Touzani, R.; Mouslim, M.; Warad, I. Synthesis of novel $Cl_2Co_4L_6$ cluster using 1-hydroxymethyl-3,5-dimethylpyrazole (LH) ligand: Crystal structure, spectral, thermal, Hirschfeld surface analysis and catalytic oxidation evaluation. *J. Mol. Struct.* **2020**, *1199*, 126995. [[CrossRef](#)]
39. Maji, A.K.; Ghosh, B.K.; Kaur, G.; Roy Choudhury, A.; Lin, C.-H.; Ribas, J.; Ghosh, R.; Mitra, M. Synthesis, crystallographic characterization and catecholase activity of a monocopper (II) and a dimanganese (III) complex with an anionic Schiff base ligand. *Polyhedron* **2013**, *61*, 15–19.
40. Jana, A.; Aliaga-Alcalde, N.; Ruiz, E.; Mohanta, S. Structures, magnetochemistry, spectroscopy, theoretical study, and catechol oxidase activity of dinuclear and dimer-of-dinuclear mixed-valence $Mn^{III}Mn^{II}$ complexes derived from a macrocyclic ligand. *Inorg. Chem.* **2013**, *52*, 7732–7746. [[CrossRef](#)]
41. Seth, P.; Das, L.K.; Drew, M.G.B.; Ghosh, A. Synthesis, Crystal Structure, and Catecholase Activity of Three Trinuclear Heterometallic $Ni_2^{II}-Mn^{II}$ Complexes Derived from a Salen-Type Schiff Base Ligand. *Eur. J. Inorg. Chem.* **2012**, *2012*, 2232–2242. [[CrossRef](#)]
42. Guha, A.; Banu, K.S.; Banerjee, A.; Ghosh, T.; Bhattacharya, S.; Zangrando, E.; Das, D. Bio-relevant manganese (II) compartmental ligand complexes: Syntheses, crystal structures and studies of catalytic activities. *J. Mol. Catal. A Chem.* **2011**, *338*, 51–57. [[CrossRef](#)]
43. Banu, K.S.; Chattopadhyay, T.; Banerjee, A.; Mukherjee, M.; Bhattacharya, S.; Patra, G.K.; Zangrando, E.; Das, D. Mono- and dinuclear manganese (III) complexes showing efficient catechol oxidase activity: Syntheses, characterization and spectroscopic studies. *Dalton Trans.* **2009**, 8755–8764. [[CrossRef](#)] [[PubMed](#)]
44. Kaizer, J.; Barath, G.; Csonka, R.; Speier, G.; Korecz, L.; Rockenbauer, A.; Parkanyi, L. Catechol oxidase and phenoxazinone synthase activity of a manganese (II) isoindoline complex. *J. Inorg. Biochem.* **2008**, *102*, 773–780. [[CrossRef](#)]
45. Kaizer, J.; Csonka, R.; Barath, G.; Speier, G. Synthesis, properties, and catecholase-like activity of the [1, 4-di (6'-methyl-2'-pyridyl) aminophthalazine] dimanganese (II) complex, $Mn_2 (6' Me_2PAP) 2Cl_4$. *Transit. Met. Chem.* **2007**, *32*, 1047–1050. [[CrossRef](#)]
46. Majumder, A.; Goswami, S.; Batten, S.R.; El Fallah, M.S.; Ribas, J.; Mitra, S. Catalytic oxidation of 3, 5-di-tert-butylcatechol by a manganese (III) 18-azametallacrown-6 compound: Synthesis, crystal structure, fluorescence, magnetic and kinetic investigation. *Inorg. Chim. Acta* **2006**, *359*, 2375–2382. [[CrossRef](#)]
47. Blay, G.; Fernandez, I.; Pedro, J.R.; Ruiz-Garcia, R.; Temporal-Sanchez, T.; Pardo, E.; Lloret, F.; Munoz, M.C. Chemistry and reactivity of dinuclear manganese oxamate complexes: Aerobic catechol oxidation catalyzed by high-valent bis (oxo)-bridged dimanganese (IV) complexes with a homologous series of binucleating 4, 5-disubstituted-o-phenylenedioxamate ligands. *J. Mol. Catal. A Chem.* **2006**, *250*, 20–26. [[CrossRef](#)]
48. Hitomi, Y.; Ando, A.; Matsui, H.; Ito, T.; Tanaka, T.; Ogo, S.; Funabiki, T. Aerobic catechol oxidation catalyzed by a Bis (μ -oxo) dimanganese (III, III) complex via a manganese (II)– semiquinonate complex. *Inorg. Chem.* **2005**, *44*, 3473–3478. [[CrossRef](#)]
49. Mukherjee, S.; Weyhermueller, T.; Bothe, E.; Wieghardt, K.; Chaudhuri, P. Dinuclear and mononuclear manganese (IV)-radical complexes and their catalytic catecholase activity. *Dalton Trans.* **2004**, 3842–3853. [[CrossRef](#)]

50. Triller, M.U.; Pursche, D.; Hsieh, W.-Y.; Pecoraro, V.L.; Rompel, A.; Krebs, B. Catalytic Oxidation of 3,5-Di-tert-butylcatechol by a Series of Mononuclear Manganese Complexes: Synthesis, Structure, and Kinetic Investigation. *Inorg. Chem.* **2003**, *42*, 6274–6283. [[CrossRef](#)]
51. Guha, A.; Chattopadhyay, T.; Paul, N.D.; Mukherjee, M.; Goswami, S.; Mondal, T.K.; Zangrando, E.; Das, D. Radical pathway in catecholase activity with zinc-based model complexes of compartmental ligands. *Inorg. Chem.* **2012**, *51*, 8750–8759. [[CrossRef](#)]
52. Olivares, C.; Solano, F. New insights into the active site structure and catalytic mechanism of tyrosinase and its related proteins. *Pigment Cell Melanoma Res.* **2009**, *22*, 750–760. [[CrossRef](#)]
53. Nikkhahi, M.; Sourì, E.; Sarkhail, P.; Baeeri, M.; Mohammadhosseini, N. Evaluation of anti-tyrosinase activity of *Allium ursinum* extracts and their metal complexes. *Acta Sci. Pol. Technol. Aliment.* **2018**, *17*, 219–226.
54. Available online: <http://www.ccdc.cam.ac.uk/conts/retrieving.html> (accessed on 1 November 2022).
55. Titi, A.; Messali, M.; Alqurashy, B.A.; Touzani, R.; Shiga, T.; Oshio, H.; Fettouhi, M.; Rajabi, M.; Almalki, F.A.; Ben Hadda, T. Synthesis, characterization, X-ray crystal study and bioactivities of pyrazole derivatives: Identification of antitumor, antifungal and antibacterial pharmacophore sites. *J. Mol. Struct.* **2020**, *1205*, 127625. [[CrossRef](#)]
56. Choi, S.; Kim, S.; Lee, H.-J.; Lee, H. Cadmium (II) complexes containing N'-substituted N,N-bispyrazolyl ligands: The formation of 4- and 5-coordinated monomers versus 6-coordinated dimer. *Inorg. Chem. Commun.* **2014**, *44*, 164. [[CrossRef](#)]
57. APEX3; Version 2017.3-0; Bruker AXS, Inc.: Madison, WI, USA, 2017.
58. Sheldrick, G.M. *Acta Crystallogr. Sect. A Fundam. Crystallogr.* **2015**, *71*, 3.